Theoretical Considerations on the Role of Membrane Potential in the Regulation of Endosomal pH

Sheree Lynn Rybak, Frederick Lanni, and Robert F. Murphy
Department of Biological Sciences and Center for Light Microscope Imaging and Biotechnology, Carnegie Mellon University, Pittsburgh, Pennsylvania 15213 USA

ABSTRACT Na^+,K^+-ATPase has been observed to partially inhibit acidification of early endosomes by increasing membrane potential, whereas chloride channels have been observed to enhance acidification in endosomes and lysosomes. However, little theoretical analysis of the ways in which different pumps and channels may interact has been carried out. We therefore developed quantitative models of endosomal pH regulation based on thermodynamic considerations. We conclude that 1) both size and shape of endosomes will influence steady-state endosomal pH whenever membrane potential due to the pH gradient limits proton pumping, 2) steady-state pH values similar to those observed in early endosomes of living cells can occur in endosomes containing just H^+-ATPases and Na^+,K^+-ATPases when low endosomal buffering capacities are present, and 3) inclusion of active chloride channels results in predicted pH values well below those observed in vivo. The results support the separation of endocytic compartments into two classes, those (such as early endosomes) whose acidification is limited by attainment of a certain membrane potential, and those (such as lysosomes) whose acidification is limited by the attainment of a certain pH. The theoretical framework and conclusions described are potentially applicable to other membrane-enclosed compartments that are acidified, such as elements of the Golgi apparatus.

GLOSSARY

B	concentration of fixed negative charges
C	capacitance of the endosomal membrane
c_c	charged ion concentration inside the endosome
ΔG	free energy difference between inside and outside of the endosome
ΔpH	pH difference between inside and outside of the endosome
Q	net charge within the endosomal membrane

Greek symbols

β	buffering capacity of the endosome
$\Delta\Psi$	membrane potential between inside and outside of the endosome
v	volume to surface area ratio of the endosome

INTRODUCTION

Many macromolecules enter cells through invagination of the plasma membrane, a process termed *endocytosis*. During endocytosis, most ingested material is exposed to a progressively lower pH as it proceeds to lysosomes for degradation (Murphy et al., 1984; Mellman et al., 1986; Roederer et al., 1987). Acidification begins in tubulo-vesicular organelles (termed *early endosomes*) and is required for proper membrane trafficking (for reviews see Mellman et al., 1986; Murphy, 1988; Yamashiro and Maxfield, 1988). The decreased pH of early endosomes favors dissociation of many incoming receptor-ligand complexes. In the well-studied case of the low-density lipoprotein (LDL) system, dissociation at acidic pH allows LDL receptors to recycle to the plasma membrane while LDL is transferred to lysosomes. The low lysosomal pH of 4.6–5.0 (Coffey and de Duve, 1968; Ohkuma and Poole, 1978; Geisow et al., 1981) provides favorable conditions for enzymatic hydrolases required for degradation. In contrast to LDL, the iron-carrying serum protein transferrin (Tf) remains bound to its receptor at low pH. Because it recycles with its receptor to the plasma membrane, Tf can be used as a convenient probe for following acidification along the receptor-recycling pathway.

Based on measurements of transferrin acidification, cultured cell lines may be divided into two classes (Murphy, 1988; Sipe et al., 1991). The first class includes BALB/c 3T3, a murine fibroblast cell line, and A549 cells, a human epidermoid carcinoma cell line. In these lines, a minimum pH of 6.1–6.2 is observed after 5 min of Tf uptake (Sipe and Murphy, 1987; Cain et al., 1989). This rapid acidification in early endosomes is followed by slower alkalinization during recycling. Ligands destined for lysosomes are first acidified like Tf in early endosomes and then further acidified in late endosomes and lysosomes. A role for the Na^+,K^+-ATPase in generating the difference in pH between early and late endosomes has been proposed. Acidification of isolated early endosomes, but not late endosomes, was observed to be enhanced in the presence of inhibitors of the Na^+,K^+-ATPase, leading to the suggestion that the Na^+,K^+-ATPase may partially inhibit acidification of early endosomes by increasing endosomal membrane potential (Fuchs et al., 1989b). In support of this hypothesis, incubation of intact cells in ouabain, a Na^+,K^+-ATPase inhibitor, was found to result in a dramatic lowering of early endosomal pH (from near 6 to below pH 5.3) (Cain et al., 1989). Removal or inactivation of Na^+,K^+-ATPase from early endosomes was proposed to allow formation of late endosomes that can

Received for publication 8 January 1997 and in final form 28 April 1997.
Address reprint requests to Dr. Robert F. Murphy, Department of Biological Sciences, Carnegie Mellon University, 4400 Fifth Avenue, Pittsburgh, PA 15213. Tel.: 412-268-3480; Fax: 412-268-6571; E-mail: murphy@cmu.edu.

0006-3495/97/08/674/14 $2.00

further acidify. Enhanced early endosomal acidification in the presence of ouabain has also been demonstrated in Swiss 3T3 cells (Zen et al., 1992). Direct evidence for the presence of Na^+,K^+-ATPase in early endosomes from rat liver has been obtained by biochemical means (Casciola-Rosen and Hubbard, 1992), although it is unclear whether Na^+,K^+-ATPase is active in these endosomes or whether it plays a role in endosomal pH regulation in liver.

The second class of cell lines includes human erythroleukemia line K562, murine Friend erythroleukemia line Sc9, and chicken erythroblast line HD3. In these lines, Tf is acidified to pH 5.4 and alkalinization of internal Tf during recycling is not observed (van Renswoude et al., 1982; Sipe et al., 1991; Killisch et al., 1992). The endosomal pH of K562 cells is insensitive to ouabain (Sipe et al., 1991), implying that Na^+,K^+-ATPase plays no role in the regulation of endosomal pH in the second class of cell lines.

Whereas Na^+,K^+-ATPases apparently function to limit acidification in early endosomes in at least some cell types, chloride channels have been shown to enhance acidification in endosomes and lysosomes (Van Dyke, 1988; Arai et al., 1989; Fuchs et al., 1989b; Bae and Verkman, 1990; Mulberg et al., 1991; Van Dyke, 1993). Various combinations of active Na^+,K^+-ATPases and active chloride channels may be proposed to explain differences in pH between early endosomes of different cell lines and between early and late endosomes within many cell types (Murphy, 1993). However, little theoretical analysis of the ways in which different pumps and channels may interact in endosomes has been carried out to test these proposed explanations. We have therefore begun development of quantitative theoretical models of endosomal pH regulation. In this paper we describe steady-state endosomal pH predictions based on thermodynamic considerations.

METHODS

For all cases, spreadsheets were designed using Microsoft Excel Version 5. (These spreadsheets are available on the Internet at http://www.stc.cmu.edu/murphylab/projects/endosomal-pH-modeling.html.) Optimization of equations with only a single unknown (cases 1 and 2) was performed using the Excel Goal Seek procedure. In cases 3 and 4, where three unknowns were present, the value of $[Na^+]_i$ or $[K^+]_i$ was fixed, and optimization of the other two unknowns was accomplished by a modified Newton's method (results within numerical error were obtained when the fixed and free ions were exchanged). Optimization of pH_i was tied to the free energy of the H^+-ATPase and optimization of $[Na^+]_i$ or $[K^+]_i$ to the free energy of the Na^+,K^+-ATPase.

RESULTS

Initial considerations

The electrical potential that exists across the plasma membrane is referred to as the resting or membrane potential. This potential is due to an unbalanced distribution of charged molecules between the cytoplasm and extracellular medium that results in the cytoplasm being negative relative to the external environment. There is also a potential across the endosomal membrane.

There are several sources of membrane potential. The first is the Donnan potential, which arises from the diffusion of counterions in an equilibrium system where at least one type of ionized macromolecule has restricted mobility. A second source of membrane potential is the active transport of ions. Electrogenic pumps, such as the Na^+,K^+-ATPase and the H^+-ATPase, transport ions against their concentration gradients at the expense of ATP. The Na^+,K^+-ATPase generates a potential because for every three Na^+ pumped in one direction (e.g., outside the cell), only two K^+ are pumped in the other direction. In many cells the membrane potential is due mainly to a third mechanism, the leakage of ions across the plasma membrane at different rates. This type of equilibrium potential is known as a diffusion potential.

Our goal was to explore the limits of the pH gradient established at steady state when different combinations of pumps and channels are present in the endosomal membrane. Because we were interested in steady-state values, the absolute number or concentration of ion pumps or channels present in the membrane was not considered as a factor. We similarly did not consider the rate of ion pumping (or ion leakage) because pumps were assumed to act until limited by thermodynamics (e.g., the amount of free energy available via ATP hydrolysis). This requires that passive fluxes of any pumped ions be insignificant or that leaks (deviations from the steady state) be sufficiently slow that they can be corrected by additional pumping. In short, we ignored diffusion potentials.

The pH difference achievable in an endosome is limited by thermodynamic parameters as embodied in the Nernst equation defining the free energy change associated with transporting a hydrogen ion (H^+) (Nernst, 1888):

$$\Delta G = -2.3RT\Delta\mathrm{pH} + ZF\Delta\Psi \qquad (1)$$

where ΔG is the free energy difference between the inside and the outside of the endosome, R is the gas constant (8.3145 J K^{-1} mol^{-1}), T is the absolute temperature (298 K under standard conditions), ΔpH is the pH difference between the inside and the outside of the endosome ($pH_i - pH_o$), Z is the charge on the ion (+1 for H^+), F is the Faraday constant (96,494 Coulomb/mol), and $\Delta\psi$ is the membrane potential between the inside and outside of the endosome. (We use the subscripts i and o throughout to refer to the inside and outside of the endosome, respectively.) Once the amount of energy required to pump a proton into the endosome exceeds the ΔG generated by the hydrolysis of a single ATP molecule under cytoplasmic conditions, no more net proton transport into the endosome can occur. Thus a combination of electrical and chemical potential may be expected to limit endosomal acidification at steady state. As discussed above, other pumps or channels

may affect the membrane potential and may therefore affect the endosomal pH. Although we refer explicitly to endosomes in the treatment below, it should be noted that all equations apply equally to other membrane-enclosed compartments undergoing acidification, such as lysosomes and the trans-Golgi network.

Case 1: endosomes containing only H^+-ATPases

Spherical endosomes

To begin, we considered endosomes containing only H^+-ATPases (Fig. 1 *a*). As a further simplification, we considered endosomes to be spheres of uniform radius r (in centimeters). To express $\Delta\psi$ in terms of pH, we start by treating the endosomal membrane as the dielectric layer of a capacitor:

$$V = Q/C \tag{2}$$

where V is the voltage across a membrane, Q is the net charge contained inside that membrane (e.g., an endosome), and C is the capacitance of the membrane (amount of charge required to give a unit voltage difference). Lipid bilayer membranes and plasma membranes have been shown to have a specific capacitance (C_o) of ~ 1 $\mu F/cm^2$ (Fricke, 1925; Cole and Curtis, 1938; Fenwick et al., 1982); this enables determination of capacitance for membrane vesicles by multiplication of the surface area by C_o. For spherical endosomes,

$$C = 4\pi r^2 C_o \tag{3}$$

We will use $C_0 = 1$ $\mu F/cm^2$ for all subsequent analysis. The total charge Q contained within an endosome is given by the difference in positive and negative ion concentrations, multiplied by the volume of the endosome:

$$Q = (H_i - OH_i)\frac{4}{3}\pi\left(\frac{r}{10}\right)^3 F$$
$$Q = \left(10^{-pH_i} - \frac{K_w}{10^{-pH_i}}\right)\frac{4}{3}\pi\left(\frac{r}{10}\right)^3 F \tag{4}$$

where pH_i is the pH inside the endosome and K_w is the ionization constant for water ($-\log_{10}K_w \approx 14$ at 25°C). In this equation, r (cm) is converted to decimeters, so that the volume is expressed in liters. We combine Eqs. 2, 3, and 4 to obtain an expression for the membrane potential,

$$\Delta\Psi = V = Q/C = \left(10^{-pH_i} - \frac{K_w}{10^{-pH_i}}\right)\frac{rF}{3000C_o} \tag{5}$$

and insert into Eq. 1 to obtain an expression for ΔG as a function of pH,

$$-\Delta G_{ATP} = -2.3RT(pH_i - pH_o) + \frac{rF^2}{3000C_o}\left(10^{-pH_i} - \frac{K_w}{10^{-pH_i}}\right) \tag{6}$$

By substitution of various values for pH_i, we can identify that value which yields a ΔG corresponding to the hydrolysis of a single ATP. Values of $\Delta G°$ for ATP hydrolysis in the literature range from -31.5 kJ/mol to -36.8 kJ/mol (Alberty, 1968; Rosing and Slater, 1972; Guynn and Veech, 1973; Alberty and Goldberg, 1992). Values of ΔG for ATP hydrolysis in vivo range from -52 kJ/mol to -64.72 kJ/mol (Veech et al., 1979; Freeman et al., 1983; Masuda et al., 1990; Dobson and Headrick, 1995); we have chosen to use -52 kJ/mol. Assuming an external (cytoplasmic) pH of 7.0 (Hannan and Wiggins, 1976; Rogers et al., 1983), the steady-state endosomal pH that is obtainable if only the H^+-ATPase is present in the endosomal membrane is shown in Fig. 2 *a* for various values of r. The size of the endosome has a significant effect on the steady-state endosomal pH obtainable in that smaller endosomes are predicted to achieve a lower pH than larger endosomes. This is due to the fact that decreasing the size of the endosome increases the surface-to-volume ratio, reducing the membrane potential for a given net charge density (see Fig. 2 *a*). This allows the chemical potential (pH gradient) to be a larger fraction of the total potential at steady state.

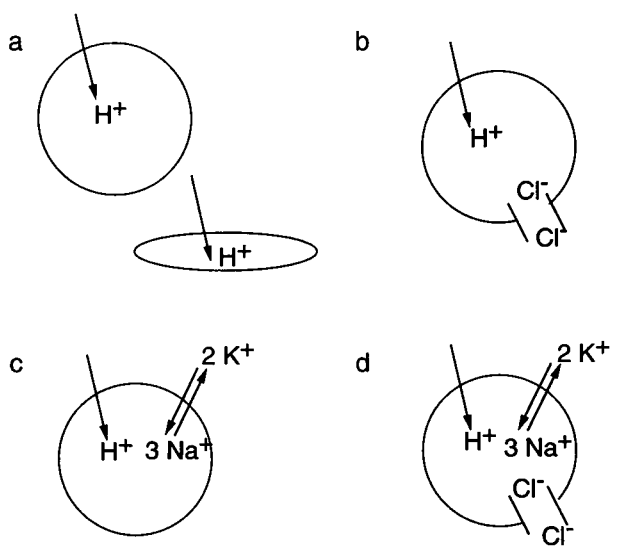

FIGURE 1 Illustration of various combinations of H^+-ATPases, Na^+,K^+-ATPases, and chloride channels considered for modeling of endosomal pH.

Prolate ellipsoidal endosomes

Because endosomes are not spherical (Helenius et al., 1983; Marsh et al., 1986; Zeidel et al., 1992; Stoorvogel et al., 1996), we next considered the effect of shape on endosomal pH. We first generalize the equations above to endosomes of arbitrary shape. To do so, we recognize that C is proportional to endosomal surface area (see Eq. 3) and Q is proportional to endosomal volume (see Eq. 4). Equation 5

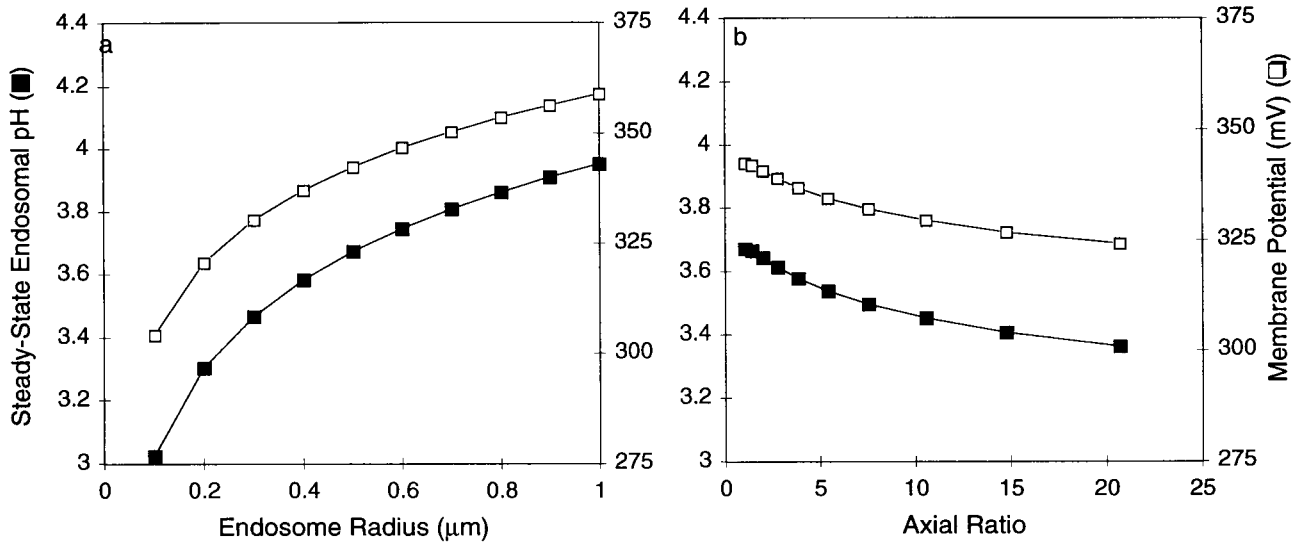

FIGURE 2 Endosome size and shape are predicted to affect both the steady-state endosomal pH and membrane potential in endosomes considered to contain only H^+-ATPases. (*a*) The steady-state endosomal pH (■) and membrane potential (□) established in spherical endosomes were predicted, using Eq. 6 as described in the text. Note that smaller endosomes are predicted to acidify to a greater extent than larger endosomes. (*b*) To examine the effect of shape on prolate ellipsoid endosomes, the axial ratio was varied while the volume was kept constant at 5.2×10^{-13} cm^3 (the volume of a sphere of 0.5-μm radius). Both the membrane potential (□) and the steady-state endosomal pH (■) predicted by Eqs. 7–9 decrease as the axial ratio of the prolate ellipsoid increases.

may therefore be rewritten as

$$\Delta\Psi = \frac{\upsilon c_c F}{1000 C_o} \tag{7}$$

where υ is the volume-to-surface area ratio (in centimeters) of the endosome (note that $\upsilon = r/3$ for spheres), and introducing c_c as the charged ion concentration, given by

$$c_c = 10^{-pH_i} - \frac{K_w}{10^{-pH_i}} \tag{8}$$

in this case. Equation 6 can then be rewritten as

$$-\Delta G_{ATP} = -2.3RT(pH_i - pH_o) + \frac{\upsilon c_c F^2}{1000 C_o} \tag{9}$$

Note that Eqs. 7 and 9 apply in the general case of an endosome of any size and shape and any ion distribution.

To model the transition between a sphere and an elongated tubule, we considered endosomes as prolate ellipsoids (Fig. 1 *a*). For prolate ellipsoids, the volume-to-surface area ratio is

$$\upsilon = \frac{(4/3)\pi ab^2}{2\pi b^2 + 2\pi ab\,(\sin^{-1}\epsilon/\epsilon)} = \frac{2ab}{3b + 3a\,(\sin^{-1}\epsilon/\epsilon)} \tag{10}$$

where a and b are, respectively, the major and minor axes of the ellipsoid (in centimeters), and ϵ, the eccentricity of the ellipsoid, is defined as

$$\epsilon = \frac{\sqrt{a^2 - b^2}}{a} \tag{11}$$

Combining Eqs. 8, 9, and 10, we obtain a free energy equation for a prolate ellipsoid analogous to Eq. 6. As before, we substituted different values of pH_i to identify the value that yields a ΔG corresponding to the hydrolysis of a single ATP. To isolate effects of shape, calculations were done for prolate ellipsoids of constant volume, but with varying ratios of major and minor axes (axial ratio). As shown in Fig. 2 *b*, the larger the axial ratio, and therefore the greater the surface area, the lower the predicted steady-state endosomal pH obtainable. This is due to the greater capacitance per unit contained volume.

Buffering capacity and Donnan potential

During endocytosis, charged membrane-impermeant macromolecules contained in the extracellular medium become enclosed inside endocytic vesicles and reach endosomes. The ionizable groups on these soluble macromolecules, as well as on membrane proteins and lipids, can buffer changes in endosomal pH and can give rise to a Donnan potential due to the diffusion of counterions into or out of the endosome (Donnan, 1925). It has been observed that membrane vesicle contents act roughly as an ampholyte, in which the number of protons required to change the pH by a fixed amount is constant over a wide pH range (Langridge-Smith and Dubinsky, 1986). In this case, the contents are described as having a fixed buffering capacity. We can therefore describe the concentration of charged macromolecules present in an endosome at a given pH as

$$c_b = -B - \beta(pH_i - pH_o) \tag{12}$$

where B is the concentration of negative fixed charges (the net concentration of ionizable groups on content macromolecules that are negatively charged) at the external (cytoplasmic) pH and β is the buffering capacity of the contents (Eq H^+/liter/pH unit).

Equation 8 may now be rewritten to include macromolecular content contributions to the total charge inside the endosome:

$$c_c = 10^{-pH_i} - \frac{K_w}{10^{-pH_i}} - B - \beta(pH_i - pH_o) \qquad (13)$$

Inserting this value and $v = r/3$ into Eq. 9 gives a free energy equation for a spherical endosome. To use this equation, we must determine values for β and B. As an estimate for β, we use the buffering capacity of tracheal apical membrane vesicles, ~50 mEq H^+/liter/pH unit (Langridge-Smith and Dubinsky, 1986). B can be calculated from measurements of the Donnan potential observed when no pumps are active. To do so, we convert the Donnan potential to a Donnan ratio, r_D, using

$$\Delta\Psi_D = \left(\frac{-RT}{F}\right)\ln r_D \qquad (14)$$

and then calculate the macromolecule concentration that corresponds to this Donnan ratio for the salt concentration, s, at which it was measured:

$$r_D = B/2s + \left[1 + \left(\frac{B}{2s}\right)^2\right]^{1/2} \qquad (15)$$

Estimates of the Donnan potential of endosomes range from −22 mV to −37 mV (Van Dyke and Belcher, 1994). These correspond to Donnan ratios of 2.36 and 4.22, which yield fixed charge concentrations of 270 mM and 558 mM (for a salt concentration of 140 mM). These values are somewhat higher than those for sarcoplasmic reticulum vesicles (84–140 mM; Yamamoto and Kasai, 1980), and tracheal apical membrane vesicles (36.5–39 mM; Langridge-Smith and Dubinsky, 1985). The fixed negative charge concentration of lysosomes has been estimated to be 230 mM (Goldman and Rottenberg, 1973).

Fig. 3 shows endosomal pH values predicted using Eqs. 9 and 13 for various values of B and β. When fixed charge values other than 0 are considered, the predicted endosomal pH values are lower than those in Fig. 2 *a* for all but the highest values of buffering capacity. Because fixed negative charges will always be masked by internalization of an equivalent amount of positive counterion during endocytosis (and because under the current assumptions the endosome is considered to be permeable only to H^+ and OH^-), nonzero values of B will not be relevant until Na^+ and K^+ fluxes are considered (cases 3 and 4). As can also be seen in Fig. 3, the predicted endosomal pH rises dramatically as the buffering capacity increases to the value observed in tracheal apical membrane vesicles (50 mEq H^+/liter/pH unit). The conclusion is that endosomes containing only H^+-ATPases will not be able to acidify significantly if their contents have buffering capacity in this range. We also note for future reference that a pH in the range of 5.4 (similar to that observed in early endosomes from K562 cells) is predicted for spherical endosomes with a buffering capacity of 0.15 mEq H^+/liter/pH unit, whereas a pH in the range of 6.2 (similar to that observed in early endosomes from A549 cells) is predicted for a buffering capacity of 0.5 mEq H^+/liter/pH unit.

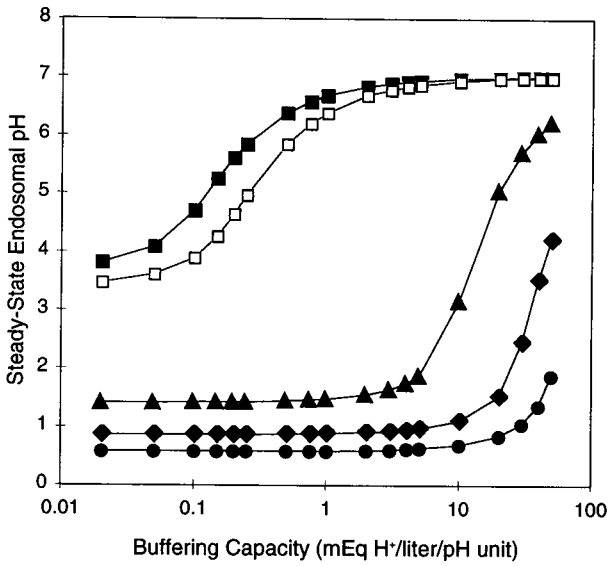

FIGURE 3 Fixed negative charge concentration and buffering capacity are predicted to dramatically affect steady-state endosomal pH. The steady-state endosomal pH was predicted for spherical endosomes containing different concentrations of fixed negative charge (■, 0 mM; ▲, 39 mM; ◆, 140 mM; ●, 270 mM) as a function of buffering capacity, by Eqs. 8, 9, and 13. Values for more elongated endosomes (v decreased by half) are also shown for 0 mM fixed negative charge (□). As buffering capacity increased, the membrane potential was predicted to increase from 351 mV to 538 mV for B = 0, from 209 mV to 492 mV for B = 39 mM, from 176 mV to 373 mV for B = 140 mM, and from 159 mV to 236 mV for B = 270 mM.

As was observed in the absence of buffering capacity (Fig. 2), a decrease in v (decrease in radius or increase in axial ratio) results in a decrease in predicted steady-state endosomal pH for buffering capacities that permit some acidification (Fig. 3).

Case 2: endosomes containing both H^+-ATPases and chloride channels

Spherical endosomes

Next we considered endosomes containing both H^+-ATPases and active chloride channels (Fig. 1 *b*). Even though we assumed that chloride could freely diffuse through the membrane via the channels, a nonzero $\Delta\Psi$ is still expected because of the balance of electrostatic and concentration-gradient driving forces. We wish to express the concentration of chloride inside the endosome (Cl_i^-) in

terms of the proton gradient and the chloride concentration outside the endosome (Cl_o^-). The free energy equations for H^+ and Cl^- are

$$0 = RT \ln \frac{Cl_i}{Cl_o} - F\Delta\Psi \tag{16}$$

$$-\Delta G_{ATP} = RT \ln \frac{H_i}{H_o} + F\Delta\Psi \tag{17}$$

Eliminating $\Delta\Psi$, we obtain

$$\frac{H_iCl_i}{H_oCl_o} = e^{(-\Delta G_{ATP}/RT)}$$
$$Cl_i = \frac{H_oCl_o}{H_i} e^{(-\Delta G_{ATP}/RT)} \tag{18}$$

The charged ion concentration term for an endosome containing both H^+-ATPases and chloride channels is then

$$c_c = 10^{-pH_i} - \frac{K_w}{10^{-pH_i}} - B - \beta(pH_i - pH_o) - \frac{10^{-pH_o}Cl_o}{10^{-pH_i}} e^{(-\Delta G_{ATP}/RT)} \tag{19}$$

We assume that the unit capacitance does not change for endosomes containing H^+-ATPases and chloride channels. We can therefore substitute Eq. 19 into Eq. 9 to obtain a free energy equation for this case.

We began our examination of this equation by determining the effect of cytoplasmic chloride concentration on the predicted pH of spherical endosomes of fixed radius (0.5 μm). Literature values for cytoplasmic chloride range from 5 mM to 50 mM (for examples see Festen et al., 1983; Abraham et al., 1985; Fitz and Scharschmidt, 1987). As shown in Fig. 4 *a*, increasing cytoplasmic chloride concentration (without considering fixed charges and buffering capacity) is predicted to cause a decrease in both membrane potential and the steady-state endosomal pH. This decrease is rapid in the range of 0–1 mM chloride, whereas increasing the concentration further has a much smaller predicted effect. The predicted endosomal chloride concentration increases dramatically as the cytoplasmic chloride concentration increases (Fig. 4 *a*, *inset*). We next varied the endosome radius while holding the chloride concentration constant at values above 1 mM. Essentially no effect on the steady-state endosomal pH or the membrane potential was seen (data not shown), in contrast to the size effects predicted for endosomes containing only H^+-ATPases. This is not surprising,

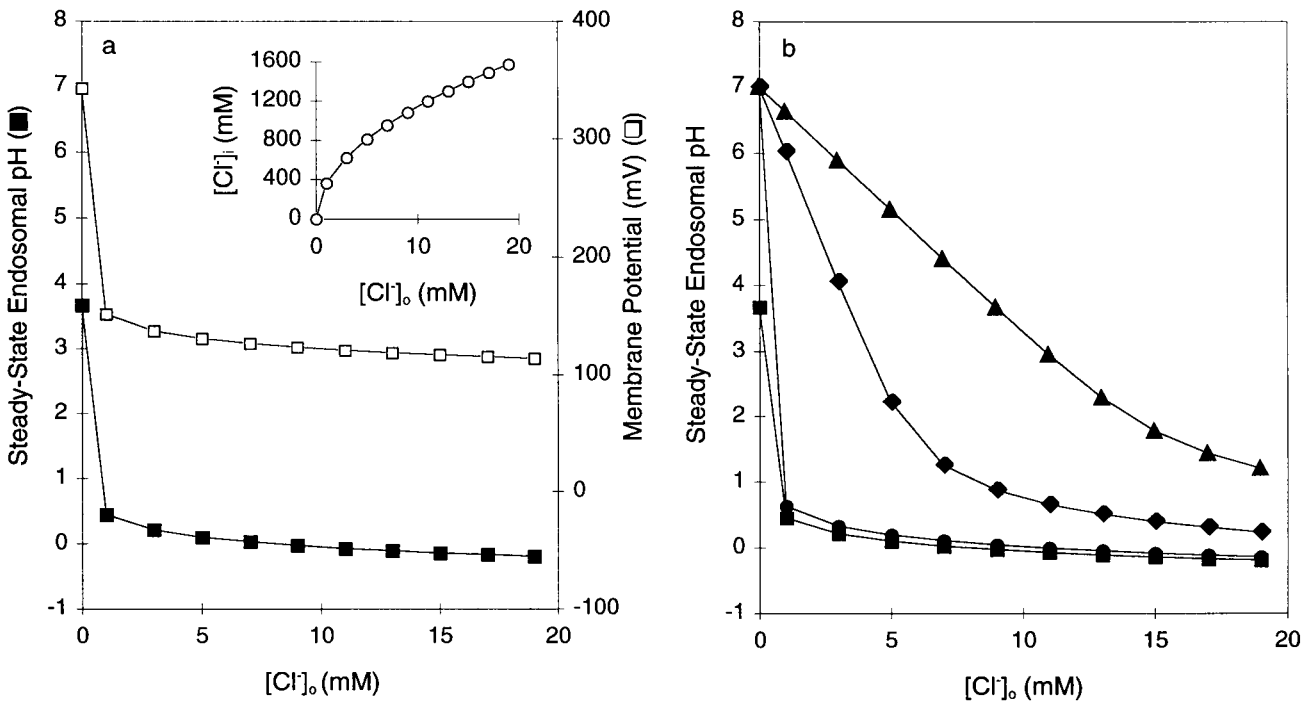

FIGURE 4 Predicted steady-state endosomal pH and membrane potential decrease dramatically when spherical endosomes are considered to contain active chloride channels in addition to H^+-ATPases. For this example, a spherical endosome with a radius of 0.5 μm was considered. (*a*) The steady-state endosomal pH (■) and the membrane potential (□) were predicted by Eqs. 7, 9, and 19 as described in the text. (*Inset*) Predicted endosomal chloride concentration. (*b*) The steady-state pH was predicted by Eq. 9 and either Eq. 19 or Eq. 21 with (●, ♦, ▲) or without (■) a 50 mEq H^+/liter/pH unit buffering capacity and with (▲, ♦) or without (■, ●) voltage gating (closing) of the chloride channel at 75 mV (▲) or 100 mV (♦). The membrane potential with no chloride was 538 mV for all conditions when buffering capacity was 50 mEq H^+/liter/pH unit. As cytoplasmic chloride concentration increased to 19 mV, the predicted membrane potential decreased to 117 mV without voltage gating, to 196 mV with voltage gating at 75 mV, and to 139 mV with voltage gating at 100 mV.

because the size and shape effects observed above were due to alterations in membrane potential, whereas membrane potential makes a relatively minor contribution to the overall free energy when chloride channels and chloride are present (for $r = 0.5$ μm and $[Cl]_o = 5$ mM, the electrical potential term represents only 24% of the overall free energy, compared to 64% when chloride is not present). To summarize, in endosomes containing H^+-ATPases and chloride channels, the presence of millimolar cytoplasmic chloride is predicted to result in an extremely low cytoplasmic pH that is unaffected by size and shape.

We also considered the effects of buffering capacity. As shown in Fig. 4 *b*, there is little difference in the predicted endosomal pH when a buffering capacity of 50 mEq H^+/liter/pH unit is used for all chloride concentrations of at least 1 mM. As discussed above, nonzero values of the fixed negative charge concentration (B) are not relevant here because of the presumed presence of (impermeable) counterions.

A number of different types of chloride channels have been described, and the exact properties of those that may be involved in endosomal and lysosomal pH regulation are uncertain (Franciolini and Petris, 1990; Jentsch et al., 1995). Some chloride channels show voltage gating, or a dependence of their probability of being open on the membrane potential. For example, ClC-1 is almost completely inactivated at (plasma) membrane potentials of −200 mV (Pusch et al., 1994). We can incorporate voltage dependence into the model by deriving an alternative equation for $[Cl^-]_i$ to replace Eq. 18. To do so we consider that point during endosome acidification at which the membrane potential reaches the cutoff voltage for the chloride channel ($\Delta\Psi_{off}$). If we assume an infinitely sharp cutoff at this voltage (i.e., no further internal chloride accumulation occurs as the voltage exceeds the cutoff), and assume that chloride ion equilibrates more rapidly than the membrane potential changes, Eq. 16 should apply at the cutoff voltage, so that

$$Cl_i = Cl_o e^{(F\Delta\Psi_{off}/RT)} \tag{20}$$

and

$$c_c = 10^{-pH_i} - \frac{K_w}{10^{-pH_i}} - B - \beta(pH_i - pH_o) - Cl_o e^{(F\Delta\Psi_{off}/RT)} \tag{21}$$

Gating of chloride channels has been extensively examined in *Xenopus* oocytes. The fast gating component of ClC-0 is completely inactivated at a plasma membrane potential of −75 mV (which corresponds to an endosomal membrane potential of +75 mV) in the presence of 0.22–1 mM extracellular chloride (Pusch et al., 1995), whereas ClC-2 is inactivated at plasma membrane potentials ranging from −100 to +50 mV (this corresponds to endosomal membrane potentials of −50 to +100 mV) (Thiemann et al., 1992). When Eq. 21 is used in place of Eq. 19 and with a cutoff voltage of 75 mV or 100 mV, we observe a dramatic increase in the predicted endosomal pH (Fig. 4 *b*). The effect of the chloride channel in this case is to allow the H^+-ATPase to at least partially overcome the buffering capacity (negligible acidification is predicted for a buffering capacity of 50 mEq H^+/liter/pH unit in the absence of active chloride channels).

Case 3: endosomes containing H^+-ATPases and Na^+,K^+-ATPases

In the third case we considered endosomes containing H^+-ATPases and Na^+,K^+-ATPases (Fig. 1 *c*). Modification of Eq. 13 to include both the Na^+ and K^+ contributions to charge gives

$$c_c = H_i - OH_i - B - \beta(pH_i - pH_o) + Na_i + K_i \tag{22}$$

Inserting this into Eq. 9 we obtain

$$\Delta G_{Hpump} = -2.3RT(pH_i - pH_o) + \frac{\upsilon F^2}{1000C_o} \times \left(10^{-pH_i} - \frac{K_w}{10^{-pH_i}} - B - \beta(pH_i - pH_o) + Na_i + K_i\right) \tag{23}$$

We now consider the energetics of the Na^+,K^+-ATPase. The free energy change for pumping three Na^+ into and two K^+ out of the endosome is

$$\Delta G_{NaKpump} = 3\left(RT\ln\frac{Na_i}{Na_o} + F\Delta\Psi\right) - 2\left(RT\ln\frac{K_i}{K_o} + F\Delta\Psi\right) \tag{24}$$

Simplifying Eq. 24 and substituting for $\Delta\Psi$ by using Eqs. 7 and 22, we obtain an expression for the free energy of ATP hydrolysis for the Na^+,K^+-ATPase:

$$\Delta G_{NaKpump} = 3RT\ln\frac{Na_i}{Na_o} - 2RT\ln\frac{K_i}{K_o} + \frac{\upsilon F^2}{1000C_o} \times \left(10^{-pH_i} - \frac{K_w}{10^{-pH_i}} - B - \beta(pH_i - pH_o) + Na_i + K_i\right) \tag{25}$$

We now have two free energy equations: one for the H^+-ATPase (Eq. 23) and one for the Na^+,K^+-ATPase (Eq. 25). To solve these two equations simultaneously, we searched for concentrations of H^+_i, Na^+_i, and K^+_i that make ΔG for both the H^+-ATPase (Eq. 23) and for the Na^+,K^+-ATPase (Eq. 25) equal to $-\Delta G_{ATP}$. We performed this search by holding either $[K^+]_i$ or $[Na^+]_i$ constant and varying the other ion concentrations. As before, we considered spherical endosomes with a radius of 0.5 μm. In addition, we assumed a $[K^+]_o$ of 150 mM and a $[Na^+]_o$ of 15 mM. These are well within reported cytoplasmic concentrations (for examples, see Hazelton and Tupper, 1981; Festen et al., 1983; Abraham et al., 1985). We began our search for solutions by using reported extracellular potassium (~5 mM) and sodium (~150 mM) values for $[K^+]_i$ and $[Na^+]_i$ (Bernstein, 1954; Anwer and Hegner, 1983). We did so because extracellular fluid present in endocytic vesicles delivered to endosomes may be expected to comprise

the major portion of the endosomal volume, and therefore the starting ion concentrations of the endosome may be hypothesized to be similar to the extracellular environment. However, no solutions are possible unless $[Na^+]_i$ is less than 0.5 mM, because the free energy for pumping sodium alone (not considering protons or potassium) exceeds the free energy of ATP hydrolysis otherwise. We therefore searched for solutions by using submillimolar concentrations of endosomal sodium and potassium. The predicted solutions of Eqs. 23 and 25 for $\beta = 0$ are shown in Fig. 5 *a*. As $[K^+]_i$ increases below 0.05 mM, the predicted $[Na^+]_i$ increases with a corresponding increase in the steady-state endosomal pH. However, as the $[K^+]_i$ increases above 0.05 mM, the predicted $[Na^+]_i$ decreases, but the steady-state endosomal pH continues to increase above pH 5.4.

When a buffering potential of 50 mEq H^+/liter/pH unit was considered (data not shown), no acidification was predicted (as was observed for H^+-ATPase alone in Fig. 3 with $B = 0$). Recalling that a buffering capacity of 0.15 mEq H^+/liter/pH unit was predicted (Fig. 3) to yield an endosomal pH of 5.4 for the case of H^+-ATPase only, we considered the effect when Na^+,K^+-ATPase was also present. As seen in Fig. 5 *a*, a narrower range of endosomal pH values is predicted for this buffering capacity, and a pH of 6.0–6.2 is predicted for a $[K^+]_i$ near 0.1 mM.

The results in Fig. 5 *a* do not consider the presence of fixed negative charge. Unlike in cases 1 and 2 above, fixed negative charge must be considered because the counterions most likely to neutralize that charge during endocytosis are H^+, Na^+, and K^+ (all of which we now consider as permeable). We therefore consider two conditions: 1) the presence of 39 mM macromolecular fixed negative charge alone, and 2) the presence of a mixture of fixed negative charge and chloride ion (Cl^- is not considered to be permeable at this point) totaling 155 mM (the combined concentration of Na^+ and K^+ in the extracellular medium). As shown in Fig. 5 *b*, solutions of Eqs. 23 and 25 are now possible over a physiological range of K^+ concentrations, but Na^+ concentrations are limited to less than 5 mM for $B = 39$ mM and less than 25 mM for $B = 155$ mM. It is interesting to compare this condition with case 1 for a buffering capacity of 50 mEq H^+/liter/pH unit and $B = 0$ (Fig. 3), where essentially no acidification was observed. It is also worth noting that a pH of 5.6–5.7 is predicted for a $[K^+]_i$ of 67 mM, the only published estimate of endosomal potassium concentration (Van Dyke, 1995).

The mechanism of acidification in this condition bears further examination. Allowing Na^+ and K^+ to equilibrate across the membrane unmasks the fixed negative charge present in the endosome and allows a pH gradient to par-

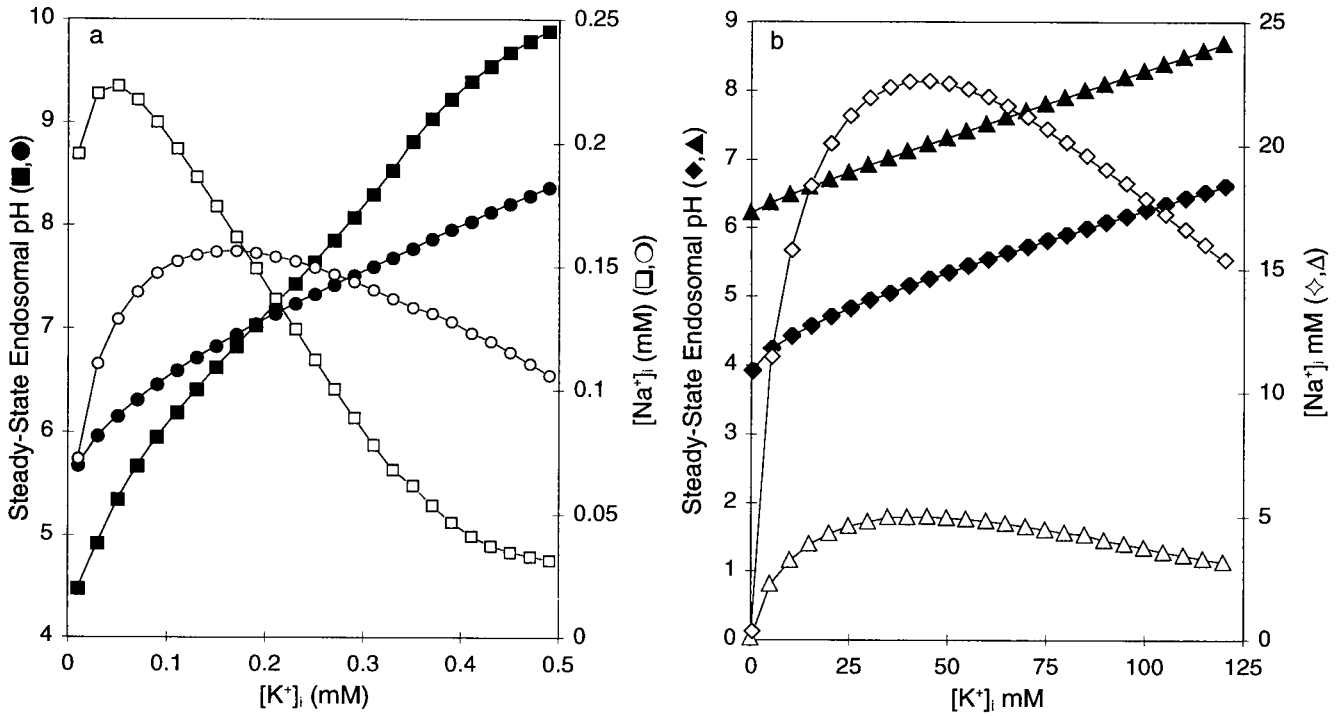

FIGURE 5 Steady-state endosomal pH is predicted to be sensitive to changes in endosomal Na^+ and K^+ concentrations when endosomes are considered to contain active H^+-ATPases and Na^+,K^+-ATPases. Spherical endosomes with a radius of 0.5 μm were considered with cytoplasmic concentrations of 150 mM for K^+ and 15 mM for Na^+. (*a*) Steady-state endosomal pH values (■, ●) and $[Na^+]_i$ values (□, ○) were predicted by Eqs. 23 and 25 with (○, ●) or without (□, ■) a buffering capacity of 0.15 mEq H^+/liter/pH unit. The predicted membrane potential increased from 385 mV to 715 mV as $[K^+]_i$ increased. (*b*) Introduction of fixed negative charge. Steady-state endosomal pH values (▲, ◆) and $[Na^+]_i$ values (△, ◇) were calculated by Eqs. 26 and 27 in the presence of a buffering capacity of 50 mEq H^+/liter/pH unit and in the presence of 39 mM (▲, △) or 155 mM (◆, ◇) fixed negative charge. As $[K^+]_i$ increased, the predicted membrane potential increased from 487 mV to 643 mV for $B = 39$ mM and from 351 mV to 521 mV for $B = 155$ mM.

tially replace a Na^+ gradient, but the presence of active Na^+,K^+-ATPase limits this replacement (preventing the pH from decreasing to the low value seen for a buffering capacity of 50 mEq H^+/liter/pH unit and $B = 155$ mM in Fig. 3). Under these conditions, the pH gradient contributes a very small part of the total electrical potential (data not shown), and thus the pH is insensitive to changes in v ($[Na^+]_i$ and $[K^+]_i$ remain sensitive to v, however). Consistent with the predictions of the model, an enhanced acidification due to Na^+ efflux has been observed in purified rat liver endosomes (Fuchs et al., 1989a) and in isolated rabbit reticulocyte endocytic vesicles (Gaete et al., 1991). In rabbit reticulocyte endosomes, the Na^+ efflux was reduced in the presence of ATP (presumably because of the action of the Na^+,K^+-ATPase) (Gaete et al., 1991). Acidification driven by Na^+ efflux has also been observed by Van Dyke (1995) in purified early, but not late, rat liver endocytic vesicles. It is important to note that the Na^+ efflux does not have to be directly coupled with H^+ influx (e.g., by an antiporter), but can take place via separate channels.

In summary, we predict that in endosomes containing H^+-ATPases and Na^+,K^+-ATPases, endosomal K^+ and Na^+ concentrations strongly influence the steady-state endosomal pH as long as the buffering capacity and/or fixed charge concentrations are such that acidification can occur at all. In addition, the predicted membrane potential is sensitive to changes in K^+ and Na^+ endosomal concentrations, with the same trend as observed for the predicted steady-state endosomal pH.

Case 4: endosomes containing H^+-ATPases, chloride channels, and Na^+,K^+-ATPases

In the fourth and final case we considered endosomes containing H^+-ATPases, active chloride channels, and Na^+,K^+-ATPases (Fig. 1 *d*). Addition of the expression for $[Cl^-]_i$ from Eq. 18 to Eqs. 23 and 25 yields

$$\Delta G_{H_{pump}} = -2.3RT(pH_i - pH_o) + \frac{vF^2}{1000C_o}\left(10^{-pH_i} - \frac{K_w}{10^{-pH_i}} - B - \beta(pH_i - pH_o) - \frac{10^{-pH_o}Cl_o}{10^{-pH_i}}e^{(-G_{ATP}/RT)} + Na_i + K_i\right) \quad (26)$$

and

$$\Delta G_{NK_{pump}} = 3RT\ln\frac{Na_i}{Na_o} - 2RT\ln\frac{K_i}{K_o} + \frac{vF^2}{1000C_o}\left(10^{-pH_i} - \frac{K_w}{10^{-pH_i}} - B - \beta(pH_i - pH_o) - \frac{10^{-pH_o}Cl_o}{10^{-pH_i}}e^{(-\Delta G_{ATP}/RT)} + Na_i + K_i\right) \quad (27)$$

As for case 3, we searched for $[H^+]_i$, $[Na^+]_i$, and $[K^+]_i$, which make ΔG for both the H^+-ATPase and for the Na^+,K^+-ATPase equal to $-\Delta G_{ATP}$. We considered spherical endosomes with a radius of 0.5 μm, a $[K^+]_o$ of 150 mM, a $[Na^+]_o$ of 15 mM, and a $[Cl^-]_o$ of 5 mM. The predicted solutions are shown in Fig. 6. Whereas $[Na^+]_i$ increases dramatically as $[K^+]_i$ increases modestly, the steady-state endosomal pH is predicted to be below 1 for all $[K^+]_i$, regardless of whether buffering capacity is present. This is in contrast to Fig. 5, where chloride channels are not considered to be active, and the predicted steady-state endosomal pH ranges from 4.5 to pH 8.5.

Therefore, in endosomes containing H^+-ATPases, chloride channels, and Na^+,K^+-ATPases, our model predicts that the Na^+,K^+-ATPase has little effect on either the steady-state endosomal pH or the membrane potential. Instead, the chloride channel is predicted to dominate the steady-state endosomal pH by dissipating the membrane potential and thereby enhancing acidification (Fig. 6).

DISCUSSION

The purpose for developing this model was to enable prediction of the ways in which changes in endosome size, shape, membrane protein composition, and ion content could affect steady-state endosomal pH and membrane po-

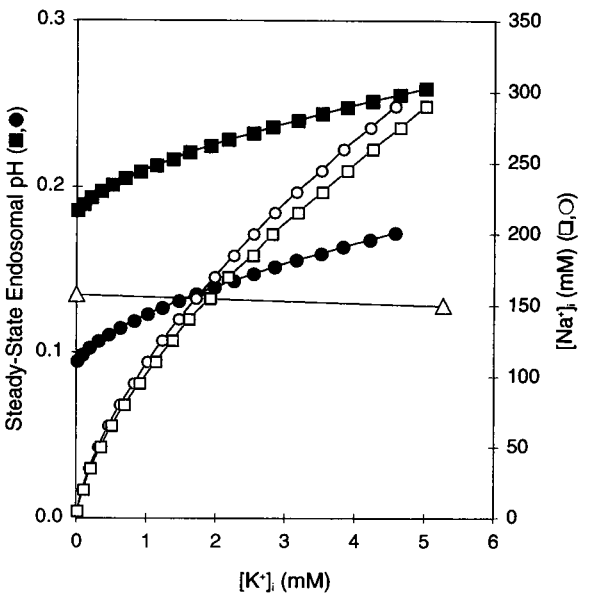

FIGURE 6 The presence of active chloride channels is predicted to overwhelm inhibition of acidification by Na^+,K^+-ATPases. Spherical endosomes with a radius of 0.5 μm were considered. With the cytoplasmic concentrations of K^+, Na^+, and Cl^- assumed to be 150 mM, 15 mM, and 5 mM, respectively. Steady-state endosomal pH values (●, ■) and $[Na^+]_i$ values (○, □) were predicted by Eqs. 26 and 27 as described in the text, in the presence (■, □) or absence (●, ○) of 50 mEq H^+/liter/pH units of buffering capacity. For reference, $[Na^+]_i$ values attainable starting at 150 mM $[Na^+]_i$, 5 mM $[K^+]_i$, assuming a 3/2 exchange for the Na^+,K^+-ATPase (and no other Na^+ or K^+ currents), are shown as a function of $[K^+]_i$ (△). Predicted values for the membrane potential were in the range of 129–137 mV and 135–142 mV, respectively, in the absence and presence of buffering capacity.

tential. The pH of endosomal compartments has been calculated from biological experimentation in several cell types (for examples see van Renswoude et al., 1982; Sipe and Murphy, 1987; Cain et al., 1989; Sipe, 1990; Sipe et al., 1991; Killisch et al., 1992). Differences in endosomal pH have been observed between cell lines of different origins, and the basis of these differences remains to be determined. Given the importance of endosomal pH for proper protein trafficking and viral infection, it would seem that these observed differences may be functionally significant.

Na^+,K^+-ATPase has been proposed to participate in endosomal pH regulation in one class of cell lines, but not in another (Sipe et al., 1991). In addition, studies have demonstrated that both the H^+-ATPase and the chloride channel can participate in endosomal pH regulation (see Introduction). However, mathematical analysis of how the H^+-ATPase, the chloride channel, or the Na^+,K^+-ATPase, and combinations thereof, may be predicted to affect endosomal pH has not been carried out. Therefore, we developed models that allowed us to compute both the steady-state endosomal pH and the membrane potential by using the Nernst equation.

Comparison of predicted pH values to known endosomal/lysosomal pH values

The predicted steady-state pH values from the model (summarized in Fig. 7) can be compared with pH values previously determined in vivo for different endocytic vesicles. From this comparison, we can make predictions about which combinations of pumps and channels may participate in pH regulation of specific organelles. For all cases described below, we considered a vesicle with a radius of 0.5 μm.

The observed early endosomal pH for one class of cell lines is pH 6.2 (for examples see Sipe and Murphy, 1987; Cain et al., 1989). Scenarios in which the model predicted a steady-state vesicular pH near 6 are as follows. First were endosomes considered to contain only H^+-ATPases (Fig. 3). Here a steady-state pH near 6 was predicted when B (concentration of fixed negative charge) was 0 with a β (buffering capacity) of ~0.5 mEq H^+/liter/pH unit or when B was 39 mM with a β of 50 mEq H^+/liter/pH unit. Second were endosomes considered to contain both H^+-ATPases and Na^+,K^+-ATPases (Fig. 5). Steady-state pH values near 6 were predicted 1) for a $[K^+]_i$ of 0.11 mM, a $[Na^+]_i$ of 0.2 mM, and no buffering capacity, 2) for a $[K^+]_i$ of 0.05 mM, a $[Na^+]_i$ of 0.13 mM, and a β of 0.15 mEq H^+/liter/pH unit, or 3) a $[K^+]_i$ of 95 mM, a $[Na^+]_i$ of 19 mM, a β of 50 mEq H^+/liter/pH unit, and a B of 155 mM. Last, endosomes considered to contain H^+-ATPases and active chloride channels were predicted to achieve a steady-state pH near 6 in the presence of 1–3 mM cytoplasmic chloride if chloride channels were voltage gated (Fig. 4 *b*).

In the second class of cell lines the observed early endosomal pH is 5.4 (van Renswoude et al., 1982; Sipe and Murphy, 1991; Killisch et al., 1992). Interestingly, scenarios that predicted a steady-state endosomal pH of 5.4 differed from those that predicted a steady-state endosomal pH of 6.2. First were endosomes considered to contain only H^+-ATPases (Fig. 3). Here a pH of 5.4 was predicted when B was 0 and β was 0.15 mEq H^+/liter/pH unit. Alternatively, if B was increased to 39 mM, a β between 20 and 30 mEq H^+/liter/pH unit predicted a vesicular pH of 5.4. Second were endosomes considered to contain both H^+-ATPases and Na^+,K^+-ATPases (Fig. 5). In this case, either a $[K^+]_i$ of 0.05 mM with a corresponding $[Na^+]_i$ near 0.22 mM without any buffering capacity or a $[K^+]_i$ of 75 mM, a $[Na^+]_i$ of 20 mM, a β of 50 mEq H^+/liter/pH unit, and a B of 155 mM were required. Last, endosomes considered to contain H^+-ATPases and active chloride channels were predicted to achieve a steady-state pH of 5.4 in the presence

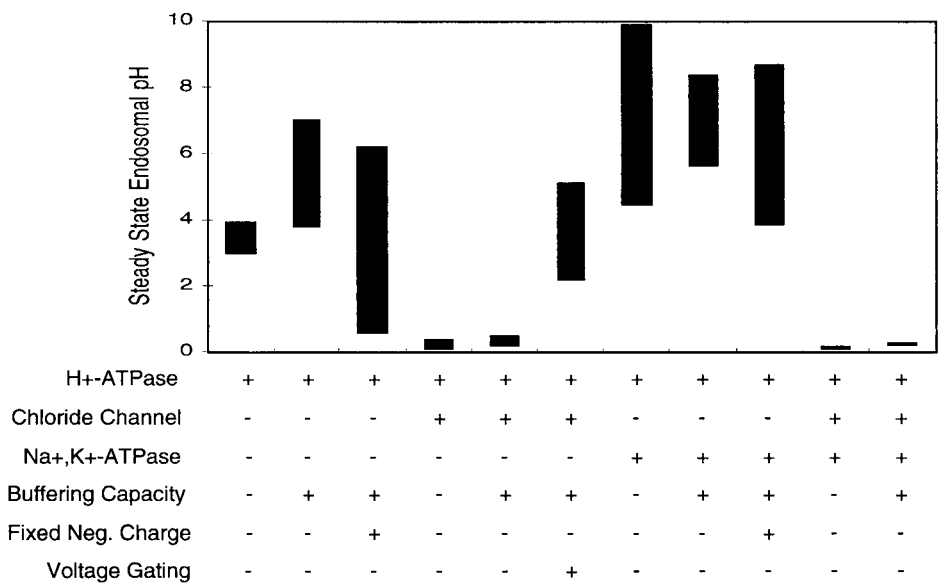

FIGURE 7 Summary of the range of predicted steady-state endosomal pH values for a vesicle with a radius of 0.5 μm when different combinations of pumps and channels are present in the endosomal membrane.

of 3–5 mM cytoplasmic chloride if the chloride channels were voltage gated (Fig. 4 *b*).

Lysosomes typically have a pH between 4 and 5 (Coffey and de Duve, 1968; Ohkuma and Poole, 1978; Geisow et al., 1981; Tycko and Maxfield, 1982). From the model we identified several scenarios that predicted a steady-state pH in this range. First were endosomes considered to contain only H^+-ATPases. As shown in Fig. 3, a B of 0 with a corresponding β between 0.05 and 0.1 mEq H^+/liter/pH unit, or a B of 39 mM with a corresponding β between 15 and 20 mEq H^+/liter/pH unit, gave steady-state pH values between 4 and 5. Second were endosomes considered to contain both H^+-ATPases and active chloride channels. A predicted steady-state pH between 4 and 5 could be achieved in the presence of 5–7 mM cytoplasmic chloride if the chloride channels were voltage gated (Fig. 4 *b*). Third were endosomes considered to contain H^+-ATPases and Na^+,K^+-ATPases. Here a β of 0 with $[K^+]_i$ between 0.01 and 0.03 mM and $[Na^+]_i$ between 0.20 and 0.22 mM gave lysosomal pH values. Any increase in β (in the presence of H^+-ATPases and Na^+,K^+-ATPases) predicted steady-state pH values above 5 unless B values greater than 39 mM were considered.

Mechanisms of pH regulation

In the scenarios described above (pH values predicted between 4 and 6.2), the model predicts that the steady-state endosomal pH is limited by chemical and/or electrical potentials. However, in no instance was a steady-state endosomal pH between pH 5.4 and pH 6.2 predicted in the presence of active, ungated chloride channels. Therefore, scenarios where steady-state pH values below 4 were predicted may be expected to be limited instead by pH dependence of H^+-ATPases or chloride channels. In the absence of such mechanisms, differences in chloride channel activity between the two classes of cell lines would not be an explanation for observed endosomal pH differences. Instead, it seems more plausible that differences in 1) concentration of negative fixed charges (B), 2) buffering capacity (β), or 3) Na^+,K^+-ATPase regulation (or combinations of these three) may be responsible for the observed endosomal pH differences in vivo.

Figs. 3 and 5 demonstrate the possible involvement of β in the regulation of steady-state endosomal pH. As shown in Fig. 3, for a fixed B, β is predicted to have dramatic effects on steady-state endosomal pH when only the H^+-ATPase is present. Therefore, if B is identical between cell lines (for example, $B = 0$), but β differs (for example, 0.5 mEq H^+/liter/pH unit for A549 cells and 0.15 mEq H^+/liter/pH unit for K562 cells), the model predicts that these two cell lines could achieve the different steady-state endosomal pH values that have been observed in vivo. As shown in Fig. 5 *a*, differences in β are also predicted to have dramatic effects on the steady-state endosomal pH when endosomes are considered to contain both H^+-ATPases and Na^+,K^+-ATPases. Therefore, if β of endosomes between the two different classes of cell lines differed, the two classes of cell lines could achieve different endosomal pH's.

Figs. 3 and 5 *a* demonstrate the predicted involvement of the Na^+,K^+-ATPase in endosomal pH regulation. In the case in which endosomes contain only H^+-ATPases (with $B = 0$ and $\beta = 0.15$ mEq H^+/liter/pH unit), an endosomal pH of 5.4 was predicted (Fig. 3). This is the early endosomal pH observed for K562 cells. When addition of the Na^+,K^+-ATPase to the endosomal membrane is considered, while keeping $B = 0$ and $\beta = 0.15$ mEq H^+/liter/pH unit, the predicted steady-state endosomal pH ranges from pH 5.7 to pH 8.3 (Fig. 5 *a*). This pH range includes the early endosomal pH for A549 cells (pH 6.2, at $[K^+]_i = 0.1$ mM), but does not include the early endosomal pH of K562 cells described above. In summary, the addition of Na^+,K^+-ATPase alone (keeping all else constant) to an endosomal membrane is a predicted mechanism by which the steady-state endosomal pH can be increased. Therefore, differences in the early endosomal pH between the two different classes of cell lines may be due to the presence or activation of Na^+,K^+-ATPases in A549 cells, but not in K562 cells. This mechanism of endosomal pH regulation between the two classes of cell lines was proposed previously (Sipe et al., 1991).

Because there are also pH differences between early endosomes and late endosomes/lysosomes, mechanisms must exist to differentially regulate the pH between these endocytic compartments. From the model, we propose the following as possible mechanisms: 1) activation of chloride channels, 2) differences in buffering capacity, and 3) differences in Na^+,K^+-ATPase localization.

The addition of active chloride channels (without voltage gating) gave predicted steady-state pH values below those observed for lysosomes (see Figs. 4 and 6). This supports previous work indicating that the introduction of active chloride channels (or activation of existing chloride channels) in the lysosomal membrane may be a mechanism by which the endosomal pH (pH ~6) can decrease to lysosomal values (pH ~5). However, chloride channels would have to be voltage gated or otherwise regulated to ensure that the pH does not fall below the reported range of 4.5–5.

In addition, as described above for early endosomal pH differences between the two classes of cell lines, changes in β may also be involved in pH differences between endosomes and lysosomes. Degradation of endosomal contents during traffic through the endocytic pathway may decrease β and result in a lower internal pH.

Another possible mechanism that can account for differences in pH between early endosomes and late endosomes/lysosomes is the inactivation or removal of Na^+,K^+-ATPases from the endosomal membrane. This hypothesis has been proposed previously (Cain and Murphy, 1988). As shown in Fig. 5 *a*, when both Na^+,K^+-ATPases and H^+-ATPases were considered, vesicles with a β of 0.15 mEq H^+/liter/pH unit and a B of 0 are predicted to obtain

steady-state pH values between 5.7 and 8.4 (pH values in the range for endosomes). However, if only H^+-ATPases are considered to be present (and assuming that β and B remain constant for endosomes and lysosomes at 0.15 mEq H^+/liter/pH unit and 0, respectively), the steady-state pH drops to 5.2.

As mentioned above, in any of the scenarios with predicted steady-state pH values below 4, acidification may be limited by pH dependence of the proton pump or the chloride channel rather than by membrane potential. This theoretical result provides support for separating endocytic compartments into those whose acidification is limited by membrane potential and those whose acidification is limited by the attainment of a specific pH. Such a fundamental difference in pH regulation was proposed previously to explain the chloroquine resistance of the CHL60-64 mutant cell line (Cain et al., 1989). We consider the effects of treatment with weak bases, such as chloroquine, on the two types of proposed compartments. Unprotonated weak bases can cross cell membranes and, upon reaching an acidic compartment, become protonated. Protonation renders the bases membrane impermeant and reduces the concentration of free protons (raising the pH). In compartments whose acidification is limited by the attainment of a specific pH (e.g., lysosomes), this should result in further proton pumping, further accumulation of weak base, and eventually, swelling of the compartment due to osmotic pressure (a process termed *vacuolation*). However, in compartments whose acidification was limited by membrane potential (e.g., early endosomes), the protonation of weak bases should not change the membrane potential, and no further proton pumping is expected, even though the pH will rise. Compartments of this type would not be expected to vacuolate. The CHL60-64 mutant has an acidification defect such that its late endosomes and lysosomes have a pH similar to that of early endosomes (Cain and Murphy, 1988). This elevated pH is thought to be due to incomplete recycling of Na^+,K^+-ATPases from early endosomes, such that some are found in late endosomes and lysosomes. Effectively, all of the endocytic compartments of CHL60-64 are similar to early endosomes. The fact that negligible vacuolation in the presence of chloroquine is observed in CHL60-64 indicates that acidification of early endosomes is indeed limited by membrane potential. On the other hand, extensive vacuolation, presumably of late endosomes and lysosomes, is observed in its parental cell line, indicating that acidification of one or both of these compartments is not.

In all of the analysis above, the capacitance per unit area of membrane was considered to be constant. As a last possible (but unlikely) mechanism of pH regulation, we can hypothesize that changes in membrane capacitance could give rise to differences in pH between endosomes and lysosomes or between endosomes of the two classes of cell lines.

Importance of vesicular shape and size in pH regulation

An interesting finding for endosomes containing only H^+-ATPases was that shape and size were predicted to strongly affect the steady-state endosomal pH and membrane potential (Fig. 2, *a* and *b*). Smaller endosomes were predicted to acidify to a greater extent than larger endosomes, and spherical endosomes were predicted to acidify to a greater extent than more elongated endosomes. In light of these observations, it is interesting to note that as endosomes fuse, their shape changes, from spherical to tubulovesicular. In addition, as endosomes mature into later compartments, their pH decreases. Further experimentation is required to determine if vesicular size and shape changes are partially responsible for changes in intravesicular pH in vivo. It is also interesting to speculate that H^+-ATPase may be actively involved in changing vesicular shape and/or volume or increasing fusion or fission. These observations are in contrast with predictions made when H^+-ATPases and active chloride channels were present. In this case the model predicted that shape and size changes have no effect on steady-state pH (data not shown).

Gating of chloride channels

Chloride channels are regulated by different gating mechanisms. Many chloride channels are voltage gated, including the ClC gene family, which to date has eight members (Jentsch et al., 1995). One member of this family is ClC-1, which has a half-maximum activation at -100 mV and is completely inactivated at -200 mV (Pusch et al., 1994). Another group of chloride channels are gated by pH. Interestingly, in frog muscle, low chloride conductance was observed at physiological pH values and above, whereas acidic pH solutions appeared to activate the channel (Warner, 1972). Still other chloride channels are gated by cytoplasmic calcium (Anderson and Welsh, 1991) or by osmotic pressure (Solc and Wine, 1991).

It is unknown at this time which of the above-described chloride channels, if any, are present in endosomal and lysosomal membranes (or whether endocytic chloride channels are as yet unidentified). If the chloride channels present in the endosomal membrane are of the type represented by ClC-2 (Thiemann et al., 1992), the slow gating component of ClC-0 (Jentsch et al., 1995), or ClC-5 (Steinmeyer et al., 1995), we do not need to consider voltage gating in modeling steady-state pH, because these channels would remain open at the membrane potentials predicted by the model (see Figs. 2–4). Alternatively, if channels of the type represented by ClC-1 (Pusch et al., 1994) or the fast gating component of ClC-0 (Pusch et al., 1995) were present in endosomes, we would need to consider voltage gating because the probability of these channels being open begins to decrease at -75 mV. We have modeled this scenario in Fig. 4 *b*. Note that gating/closing the chloride channel at 75 mV or 100 mV is predicted to increase the steady-state endoso-

mal pH to physiological values. Therefore, channels similar to ClC-1 may be good candidates for the type of chloride channel present in endosomes and lysosomes.

Limitations of the model and future directions

A potential concern regarding the results presented above is that predicted membrane potential values were quite high (greater than 300 mV) in some cases, compared to values measured for isolated endosomes and lysosomes that are less than 100 mV (for examples see Van Dyke, 1988, 1993; Van Dyke and Belcher, 1994). Further experiments will be required to determine if such high membrane potentials are observed in early endosomes. The introduction of active chloride channels resulted in a dramatic lowering of the predicted membrane potential to 100–150 mV. Although these membrane potential values are closer to measured values, they were associated with predicted steady-state endosomal pH values below 1.

The model described here can be extended by considering contributions from other ions (such as calcium) and membrane proteins (such as the Na^+-H^+ exchanger and/or the Cl^--HCO_3^- exchanger, which are found in the plasma membrane and are important for maintaining cytoplasmic pH). In addition, alternative models could be generated to consider the kinetics of pH regulation in endosomes, as has been done for renal proximal tubule (Verkman and Alpern, 1987).

CONCLUSIONS

We have described an approach that allows the prediction of steady-state endosomal pH values in the presence of different combinations of pumps and channels. This model predicts that combining different pumps and channels in the endosomal membrane results in significant differences in predicted pH and membrane potential values. It is expected that the work described here may represent a framework for evaluating experimentally derived explanations for the observed early endosomal pH differences in vivo and the pH differences between vesicles within the same cell. In addition, the model has generated predictions that may be tested through experimentation.

We thank the members of the Murphy laboratory for their helpful discussions and careful reading of the manuscript, and Alan Koretsky, David Hackney, Christopher Widnell, Neil Bradbury, Robert Bridges, Alan Verkman, and John Cuppoletti for many helpful discussions and suggestions.

This work was supported in part by a research grant from the American Heart Association, Pennsylvania Affiliate (RFM); by graduate student fellowships to SLR from the American Heart Association, Pennsylvania Affiliate; by National Science Foundation Graduate Research Traineeship Program grant BIR-9256343; and by National Science Foundation Science and Technology Center grant MCB-8920118.

REFERENCES

Abraham, E. H., J. L. Breslow, J. Epstein, P. Chang-Sing, and C. Lechene. 1985. Preparation of individual human diploid fibroblasts and study of ion transport. *Am. J. Physiol.* 248:C154–C164.

Alberty, R. A. 1968. Effect of pH and metal ion concentration on the equilibrium hydrolysis of adenosine triphosphate to adenosine diphosphate. *J. Biol. Chem.* 243:1337–1343.

Alberty, R. A., and R. N. Goldberg. 1992. Standard thermodynamic formation properties for the adenosine 5′-triphosphate series. *Biochemistry.* 31:10610–10615.

Anderson, M. P., and M. J. Welsh. 1991. Calcium and cAMP activate different chloride channels in the apical membrane of nomral and cystic fibrosis epithelia. *Proc. Natl. Acad. Sci. USA.* 88:6003–6007.

Anwer, M. S., and D. Hegner. 1983. Role of inorganic electrolytes in bile acid-independent canalicular bile formation. *Am. J. Physiol.* 244: G116–G124.

Arai, H., S. Pink, and M. Forgac. 1989. Interaction of anions and ATP with the coated vesicle proton pump. *Biochemistry.* 28:3075–3082.

Bae, H.-R., and A. S. Verkman. 1990. Protein kinase A regulates chloride conductance in endocytic vesicles from proximal tubules. *Nature.* 348: 637–639.

Bernstein, R. E. 1954. Potassium and sodium balance in mammalian red cells. *Science.* 120:459–460.

Cain, C. C., and R. F. Murphy. 1988. A chloroquine-resistant swiss 3T3 cell line with a defect in late endocytic acidification. *J. Cell Biol.* 106:269–277.

Cain, C. C., D. M. Sipe, and R. F. Murphy. 1989. Regulation of endocytic pH by the Na^+,K^+-ATPase in living cells. *Proc. Natl. Acad. Sci. USA.* 86:544–548.

Casciola-Rosen, L. A., and A. L. Hubbard. 1992. Lumenal labeling of rat hepatocyte early endosomes: presence of multiple membrane receptors and the Na^+,K^+-ATPase. *J. Biol. Chem.* 267:8213–8221.

Coffey, J. W., and C. de Duve. 1968. Digestive activity of lysosomes. *J. Biol. Chem.* 243:3255–3263.

Cole, K. S., and H. J. Curtis. 1938. Electric impedance of the squid giant axon during activity. *J. Gen. Physiol.* 22:649–670.

Dobson, G. P., and J. P. Headrick. 1995. Bioenergetic scaling: metabolic design and body-size constraints in mammals. *Proc. Natl. Acad. Sci. USA.* 92:7317–7321.

Donnan, F. G. 1925. The theory of membrane equilibria. *Chem. Rev.* 1:73–90.

Fenwick, E. M., A. Marty, and E. Neher. 1982. A patch-clamp study of bovine chromaffin cells and of their sensitivity to acetylcholine. *J. Physiol. (Lond.).* 331:577–597.

Festen, C. M. A. W., J. F. G. Slegers, and C. H. Van Os. 1983. Intracellular activities of chloride, potassium and sodium ions in rabbit corneal epithelium. *Biochim. Biophys. Acta.* 732:394–404.

Fitz, J. G., and B. F. Scharschmidt. 1987. Intracellular chloride activity in intact rat liver: relationship to membrane potential and bile flow. *Am. J. Physiol.* 252:G699–G706.

Franciolini, F., and A. Petris. 1990. Chloride channels of biological membranes. *Biochim. Biophys. Acta.* 1031:247–259.

Freeman, D., S. Bartlett, G. Radda, and B. Ross. 1983. Energetics of sodium transport in the kidney. Saturation transfer ^{31}P-NMR. *Biochim. Biophys. Acta.* 762:325–336.

Fricke, H. 1925. The electric capacity of suspensions with special reference to blood. *J. Gen. Physiol.* 9:137–152.

Fuchs, R., P. Male, and I. Mellman. 1989a. Acidification and ion permeabilities of highly purified rat liver endosomes. *J. Biol. Chem.* 264: 2212–2220.

Fuchs, R., S. Schmid, and I. Mellman. 1989b. A possible role for the Na^+,K^+-ATPase in regulating ATP-dependent endosome acidification. *Proc. Natl. Acad. Sci. USA.* 86:539–543.

Gaete, V., M. T. Nunez, and J. Glass. 1991. Cl^-, Na^+, and H^+ fluxes during the acidification of rabbit reticulocyte endocytic vesicles. *J. Bioenerg. Biomembr.* 23:147–160.

Geisow, M. J., P. D'Arcy Hart, and M. R. Young. 1981. Temporal changes of lysosome and phagosome pH during phagolysosome formation in

macrophages: studies by fluorescence spectroscopy. *J. Cell Biol.* 89: 645–652.

Goldman, R., and H. Rottenberg. 1973. Ion distribution in lysosomal suspensions. *FEBS Lett.* 33:233–238.

Guynn, R. W., and R. L. Veech. 1973. The equilibrium constants of the adenosine triphosphate hydrolysis and the adenosine triphosphate-citrate lyase reactions. *J. Biol. Chem.* 248:6966–6972.

Hannan, S. F., and P. M. Wiggins. 1976. Intracellular pH of frog sartorius muscle. *Biochim. Biophys. Acta.* 428:205–222.

Hazelton, B. J., and J. T. Tupper. 1981. Intracellular ionic changes in normal and transformed human fibroblasts after extracellular Ca^{2+} deprivation. *Biochem. J.* 194:707–711.

Helenius, A., I. Mellman, D. Wall, and A. Hubbard. 1983. Endosomes. *Trends Biochem. Sci.* 8:245–249.

Jentsch, T. J., W. Günther, M. Pusch, and B. Schwappach. 1995. Properties of voltage-gated chloride channels of the ClC gene family. *J. Physiol. (Lond.).* 482:19–25.

Killisch, I., P. Steinlein, K. Römisch, R. Hollinshead, H. Beug, and G. Griffiths. 1992. Characterization of early and late endocytic compartments of the transferrin cycle: transferrin receptor antibody blocks erythroid differentiation by trapping the receptor in the early endosome. *J. Cell Sci.* 103:211–232.

Langridge-Smith, J. E., and W. P. Dubinsky. 1985. Donnan equilibrium and pH gradient in isolated tracheal apical membrane vesicles. *Am. J. Physiol.* 249:C417–C420.

Langridge-Smith, J. E., and W. P. Dubinsky. 1986. Relationship of the Donnan potential to the transmembrane pH gradient in tracheal apical membrane vesicles. *J. Membr. Biol.* 94:197–204.

Marsh, M., G. Griffiths, G. E. Dean, I. Mellman, and A. Helenius. 1986. Three-dimensional structure of endosomes in BHK-21 cells. *Proc. Natl. Acad. Sci. USA.* 83:2899–2903.

Masuda, T., G. P. Dobson, and R. L. Veech. 1990. The Gibbs-Donnan near-equilibrium system of heart. *J. Biol. Chem.* 265:20321–20334.

Mellman, I., R. Fuchs, and A. Helenius. 1986. Acidification of the endocytic and exocytic pathways. *Annu. Rev. Biochem.* 55:663–700.

Mulberg, A. E., B. M. Tulk, and M. Forgac. 1991. Modulation of coated vesicle chloride channel activity and acidification by reversible protein kinase A-dependent phosphorylation. *J. Biol. Chem.* 266:20590–20593.

Murphy, R. F. 1988. Processing of endocytosed material. *Adv. Cell Biol.* 2:159–180.

Murphy, R. F. 1993. Models of endosome and lysosome traffic. *Adv. Cell Mol. Biol. Membr.* 1:1–17.

Murphy, R. F., S. Powers, and C. R. Cantor. 1984. Endosomal pH measured in single cells by dual fluorescence flow cytometry: rapid acidification of insulin to pH 6. *J. Cell Biol.* 98:1757–1762.

Nernst, W. 1888. Zur Kinetik der in Loesung befindlichen Koerper. *Z. Phys. Chem.* 3:613–637.

Ohkuma, S., and B. Poole. 1978. Fluorescence probe measurement of the intralysosomal pH in living cells and the perturbation of pH by various agents. *Proc. Natl. Acad. Sci. USA.* 75:3327–3331.

Pusch, M., U. Ludewig, A. Rehfeldt, and T. J. Jentsch. 1995. Gating of the voltage-dependent chloride channel ClC-0 by the permeant anion. *Nature.* 373:527–531.

Pusch, M., K. Steinmeyer, and T. J. Jentsch. 1994. Low single channel conductance of the major skeletal muscle chloride channel, ClC-1. *Biophys. J.* 66:149–152.

Roederer, M., R. Bowser, and R. F. Murphy. 1987. Kinetics and temperature dependence of exposure of endocytosed material to proteolytic enzymes and low pH: evidence for a maturation model for the formation of lysosomes. *J. Cell. Physiol.* 131:200–209.

Rogers, J., T. R. Hesketh, G. A. Smith, and J. C. Metcalfe. 1983. Intracellular pH of stimulated thymocytes measured with a new fluorescent indicator. *J. Biol. Chem.* 258:5994–5997.

Rosing, J., and E. C. Slater. 1972. The value of $\Delta G°$ for the hydrolysis of ATP. *Biochim. Biophys. Acta.* 267:275–290.

Sipe, D. M. 1990. Endosomal acidification and iron release from transferrin. Ph.D. dissertation. Department of Biological Sciences, Carnegie Mellon University, Pittsburgh, PA.

Sipe, D. M., A. Jesurum, and R. F. Murphy. 1991. Absence of Na^+,K^+-ATPase regulation of endosomal acidification in K562 erythroleukemia cells. *J. Biol. Chem.* 266:3469–3474.

Sipe, D. M., and R. F. Murphy. 1987. High resolution kinetics of transferrin acidification in BALB/c 3T3 cells: exposure to pH 6 followed by temperature-sensitive alkalinization during recycling. *Proc. Natl. Acad. Sci. USA.* 84:7119–7123.

Sipe, D. M., and R. F. Murphy. 1991. Binding to cellular receptors results in increased iron release from transferrin at mildly acidic pH. *J. Biol. Chem.* 266:8002–8007.

Solc, C. K., and J. J. Wine. 1991. Swelling-induced and depolarization-induced Cl^- channels in normal and cystic fibrosis epithelial cells. *Am. J. Physiol.* 261:C658–C674.

Steinmeyer, K., B. Schwappach, M. Bens, A. Vandewalle, and T. J. Jentsch. 1995. Cloning and functional expression of rat CLC-5, a chloride channel related to kidney disease. *J. Biol. Chem.* 270:31172–31177.

Stoorvogel, W., V. Oorschot, and H. J. Geuze. 1996. A novel class of clathrin-coated vesicles budding from endosomes. *J. Cell Biol.* 132: 21–33.

Thiemann, A., S. Gründer, M. Pusch, and T. J. Jentsch. 1992. A chloride channel widely expressed in epithelial and non-epithelial cells. *Nature.* 356:57–60.

Tycko, B., and F. R. Maxfield. 1982. Rapid acidification of endocytic vesicles containing α_2-macroglobulin. *Cell.* 28:643–651.

Van Dyke, R. W. 1988. Proton pump-generated electrochemical gradients in rat liver multivesicular bodies. *J. Biol. Chem.* 263:2603–2611.

Van Dyke, R. W. 1993. Acidification of rat liver lysosomes: quantitation and comparison with endosomes. *Am. J. Physiol.* 265:C901–C917.

Van Dyke, R. W. 1995. Na^+/H^+ exchange modulates acidification of early rat liver endocytic vesicles. *Am. J. Physiol.* 269:C943–C954.

Van Dyke, R. W., and J. D. Belcher. 1994. Acidification of three types of liver endocytic vesicles: similarities and differences. *Am. J. Physiol.* 266:C81–C94.

van Renswoude, J., K. R. Bridges, J. B. Harford, and R. D. Klausner. 1982. Receptor-mediated endocytosis of transferrin and the uptake of Fe in K652 cells: identification of a nonlysosomal acidic compartment. *Proc. Natl. Acad. Sci. USA.* 79:6186–6190.

Veech, R. L., J. W. R. Lawson, N. W. Cornell, and H. A. Krebs. 1979. Cytosolic phosphorylation potential. *J. Biol. Chem.* 254:6538–6547.

Verkman, A. S., and R. J. Alpern. 1987. Kinetic transport model for cellular regulation of pH and solute concentration in the renal proximal tubule. *Biophys. J.* 51:533–546.

Warner, A. 1972. Kinetic properties of the chloride conductance of frog muscle. *J. Physiol. (Lond.).* 227:291–312.

Yamamoto, N., and M. Kasai. 1980. Donnan potential in sarcoplasmic reticulum vesicles measured by using a fluorescent cyanine dye. *J. Biochem. (Tokyo).* 88:1425–1435.

Yamashiro, D. J., and F. R. Maxfield. 1988. Regulation of endocytic processes by pH. *Trends Pharmacol. Sci.* 9:190–193.

Zeidel, M. L., T. G. Hammond, B. Botelho, and H. W. Harris, Jr. 1992. Functional and structural characterization of endosomes from toad bladder epithelial cells. *Am. J. Physiol.* 263:F62–F76.

Zen, K., J. Biwersi, N. Periasamy, and A. S. Verkman. 1992. Second messengers regulate endosomal acidification in Swiss 3T3 fibroblasts. *J. Cell Biol.* 119:99–110.